Synthetic Jet 주위 유도 와류에 대한 수치 해석

박 수 형*[1], 사 정 환[2], 유 영 훈[1]

NUMERICAL INVESTIGATION OF VORTICAL FLOW INDUCED BY A SYNTHETIC JET ACTUATOR

S.H. Park*[1], J.H. Sa[2], and Y.H. Yu[1]

Piezoelectric actuators have been investigated for flow control in the field of fluid dynamics. Numerical simulation for a single diaphragm piezoelectric actuator operating in quiescent air is performed to investigate the complex flow field around the slot exit. A periodic velocity transpiration condition is applied to simulate the effect of the moving diaphragm. The computational results for the flow field around the slot exit agree well with the experimental data. The results also show that low pressure regions due to the vortex pairing cause non-monotonic variations in the vertical velocity.

Key Words: 전산유체역학(CFD), 비정상 난류 유동(Unsteady Turbulent Flow), 와류 상호작용(vortex interaction), Synthetic jet

1. Introduction

Synthetic jet actuators have been used to improve performance of various mechanical systems that cover a wide range from aerospace vehicles to micro-electromechanical systems (MEMS). An oscillatory motion of the diaphragm in a piezoelectric actuator generates a synthetic jet that exhausts into the surrounding air. Fluid is ejected from the cavity by the forward motion of the diaphragm. The flow separates at the sharp edges of the slot exit forming a vortex sheet that rolls into a vortex pair and begins to move away from the exit under its own self-induced velocity [1]. The time-harmonic jet interacts with couples of vortex pairs that are induced at the edge of the slot exit by the motion of a diaphragm. When the diaphragm begins to move away form the slot exit, the vortex pair is already sufficiently removed and is thus unaffected by the ambient fluid that is drawn into the cavity. Therefore, the net mass flux out of the cavity is zero whereas the aeroodynamic impulse of each vortex pair is nonzero. Unlike conventional continuous jets or pulsed jets a unique feature of synthetic jets is that they transfer linear momentum to the flow system without net mass injection across the system boundary [2]. Thus, closed recirculation flow region is generated by the interaction of synthetic jets with an external flow near the flow boundary.

Several approaches for simulations of synthetic jet actuators are found in the literature [4-5]. The main problem associated with full numerical simulations is huge computational cost. Internal flow simulation of cavity requires at least the same number of grid points needed to solve the exterior flowfield [3]. Furthermore, since the Mach number in the problem varies from O(10-3) to O(1), numerical difficulties are caused by the flow velocity variation from fully incompressible to fully compressible regimes and the modeling of the oscillating boundary [4]. Computational time and numerical complexity make it difficult to do a full numerical simulation. From this reason, simplified transpiration boundary conditions that do not simulate the flow inside the actuator cavity have been used for modeling synthetic jet flows, though the simplified boundary condition does not satisfy the conservation laws [3]. We devote special attention to establishing appropriate boundary condition for such flows, especially in the absence of the detailed experimental data

1 정회원, 건국대학교 항공우주공학과
2 학생회원, 건국대학교 항공우주공학과 대학원
* Corresponding author E-mail: pish@konkuk.ac.kr

required for closure.

The primary objectives of this paper are to develop a numerical algorithm for simulations of synthetic jets and to investigate the physical aspect of the synthetic jet. The effect of the turbulence on the jet structure with diaphragm velocity is investigated also.

2. Numerical Approach

The time-dependent compressible Navier-Stokes equations with preconditioning and the k-ω turbulence equations are considered to describe the unsteady airflow generated by a synthetic jet actuator:

$$\frac{\partial Q}{\partial t}+\frac{\partial F_i}{\partial x_i}=-\frac{\partial P}{\partial x_i}+\frac{1}{\mathrm{Re}}\frac{\partial F_{vi}}{\partial x_i}+S \qquad (1)$$

where Q is the flow variable and Fi and Fvi are the inviscid and viscous fluxes in each direction, respectively. The source term, S, is modeled for the turbulence equations. Time-derivative preconditioning techniques are used to take compressibility effect of the jet into account and to reduce convergence problems that occur at low Mach number flows [6,7]. An efficient DADI method with second-order dual-time stepping algorithm is used for the Navier-Stokes and k-ω turbulence equations with a weakly nonlinear correction that improves the performance of the turbulence model in presence of adverse pressure gradients [8].

A single diaphragm piezoelectric actuator operating in quiescent air consists of a 1.27 mm-wide rectangular slot connected to a cavity with a circular piezoelectric diaphragm [9]. The slot exit is perfectly matched to a rectangular hole in the base of the enclosure box with 600 mm long sides. Although the flow inside cavity of the actuator is highly three dimensional, the actual geometry is modeled as a two-dimensional configuration. A sectional cut at the midspan location is shown schematically in Fig. 1, showing the oscillating diaphragm and slot geometry. The diaphragm motion can be simulated via a prescribed motion imposed at the diaphragm surface located at the side of the cavity when we compute the flow without any geometrical assumption.

It can be concluded from the previous computational results [3-5] that reproducing the flow conditions at the slot exit is more important than the detailed modeling of cavity geometry for accurate simulation of a synthetic jet for this configuration. The actuator characteristic size can be evaluated as $L_a = V_a/S_a$, where Va and Sa are the actuator volume and internal surface area, respectively. The characteristic length of the actuator considered in the present study is O(10-2) m, while the wavelength of diaphragm oscillations is $\lambda = \omega/C_\infty$, where ω is the diaphragm frequency and C∞ is the speed of sound. With the diaphragm frequency of 450 Hz,

$$\frac{L_a}{\lambda}=\frac{V_a\omega}{S_aC_\infty}\approx 3\times10^{-2}<<1 \qquad (2)$$

As discussed by Yamaleev and Carpenter [4], the size of a realistic actuator is much less than the wavelength of diaphragm vibration. Their estimate implies that all changes in the pressure and velocity fields inside the actuator cavity occur under the scale of the wavelength of diaphragm vibration. This also means that the cavity shape does not significantly affect the actuator performance. Therefore, we simulated the experimental test case with simplified cavity geometry. A periodic velocity transpiration condition is applied at the bottom of the slot's neck to mimic the effect of a moving diaphragm. A simple curve-fitted temporal variation of peak velocity is proposed to replicate the velocity signal measured at the slot exit, x=0 and y=0.1 mm:

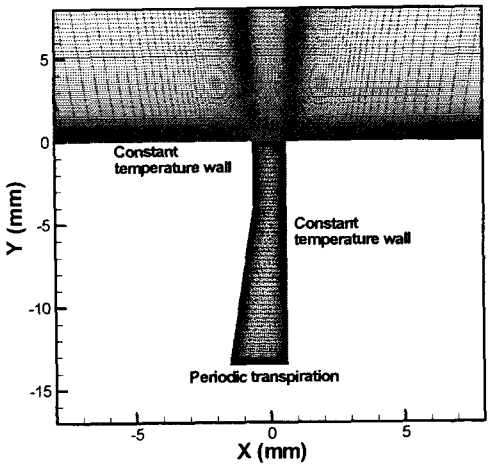

Fig.1 Schematic of piezoelectric actuator and simplified geometry

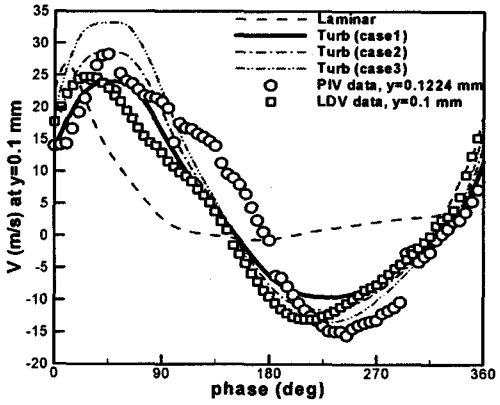

Fig. 2 Time history of V velocity near slot exit.

$$v(t)_{\max} = \frac{A}{\Theta^{0.55}} \sin(2\pi f t) \tag{3}$$

where $\Theta = \max(0.25, \theta / 2\pi)$ and A is an empirical amplitude to reproduce the peak velocity in order to reproduce experimental velocity profiles at the slot exit. The value should be determined by numerical experiments in advance before the computation is performed. The present velocity profile mimics the experimental velocity variation with phase angle θ and with a single dominant frequency (f) of 450 Hz replicating the experimental data. This transpiration condition does not satisfy the conservation laws because the pressure distribution cannot be prescribed numerically. In this study, the pressure at the boundary is simply extrapolated from the interior computational cell.

The Reynolds number is approximately 2800 based on the peak jet velocity and slot width and thus fully turbulent computations are performed for the jet simulation (discussed later). We use the same multiblock structured grid as that used by Vatsa and Turkel [3], consisting of 61,000 nodes as a baseline grid for these computations. Similarly, a finer grid (FG), consisting of approximately 250,000 nodes, was created by doubling the baseline grid in each direction. Most of the computations were performed with the two-equation Wilcox-Durbin+ (WD+) turbulence model using 144 time steps/period corresponding to 2.5 deg phase angle between the time steps [8]. To assess the effect of temporal resolution computations with half of the baseline time step were performed. The computations show that both results give little difference for the present cases.

3. BEHAVIOR OF THE SYNTHETIC JET

Several thousand cycles of diaphragm vibration are needed to generate phase-locked ensemble average data equivalent to the experimental data. Consideration of the decay rate of the vortices in the exterior chamber is helpful to determine the minimum number of the simulation cycle that is necessary to replicate the experiment. The time scale of the viscous dissipation (Kolmogorov scale) is of the order of $t_{dis} = l^2/\nu$, where l ($=1.27\times10^{-3}$ m) is the characteristic length scale of a vortex and ν ($=1.55\times10^{-5}$ m^2/s) is the kinematic viscosity. Then, the characteristic time scale of the vortex kinetic energy decay is of the order of 0.1 s. From a conclusion that the laminar viscous dissipation time scale is two orders of magnitude larger than the period of diaphragm vibration, it can be deduced that couples of vortices in the domain interact with each other for a long period of time [4]. This vortex-vortex interaction should be accurately simulated. The numerical solution is non-periodic in time during a period of diaphragm vibration, because the vortex-vortex interaction destroys the periodic behavior after a few cycles from the initial stage. Statistically significant results can be generated by integration of the solution during at least $O(10^{-1})$ seconds equivalent to the time scale of the viscous dissipation. This means $O(10^2)$ cycles of diaphragm oscillation are needed for computational time integration. See Reference [4] for more detailed discussion. Because of a huge amount of computational time required, only 30 cycles of diaphragm oscillation have been simulated and the flow variables are integrated during 20 cycles of the oscillation in this study.

Figure 2 displays the time history of V velocity near slot exit, x=0 and y=0.1 mm. There is a large variation in the experimental data. Since the performance of the piezoelectric diaphragm degrades over time, for a given input voltage, the actuator produces smaller jet velocities as it ages. Yao et al.[9] have recently acquired experimental data for this configuration with a new piezoelectric diaphragm and obtained the detailed field data with the PIV techniques. Computations with laminar

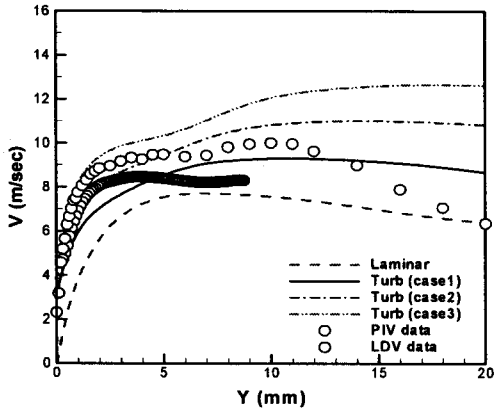

Fig. 3 Time-averaged V velocity along centerline(x=0 mm).

and turbulent assumptions were compared with the particle image velocimeter (PIV) and the laser Doppler velocimeter (LDV) data. To investigate the effect of diaphragm vibrating velocity on the synthetic jets, three cases were computed for different magnitudes of A in Eq. (3) of the diaphragm velocity (Table 1). The magnitude of A is associated with the maximum deflection of the diaphragm mounted in the piezoelectric actuator. The resulting peak velocity near the exit varies linearly with the magnitude of *A*. Laminar assumption gives a poor correlation with the experimental data, whereas all turbulent cases mimic the variation when those are compared with the magnitude of the experimental data. Among them case 2 with *A*=9.08 agrees well with PIV data from 0 to 90 degrees and with LDV data for higher phase degrees. This implies that the flow near slot exit is turbulent in this velocity regime and that the present single-harmonic transpiration boundary condition replicateswell the experimental data near the exit.

In Fig. 3, long time-averaged V velocities along centerline are

Table 1. Peak V velocity for computed cases.

Case	A	Peak V at y=0.1 mm
laminar	7.57	26.8
1	7.57 (100 %)	24.0 (100 %)
2	9.08 (120 %)	28.6 (119 %)
3	10.60 (140 %)	33.2 (138 %)

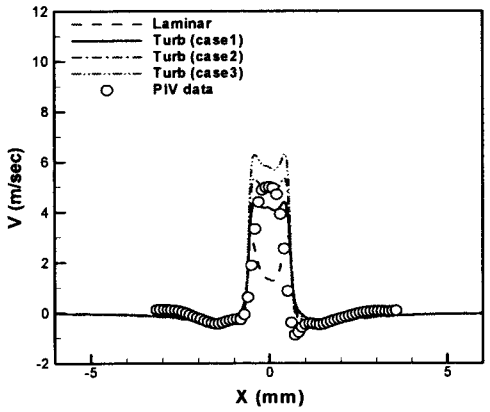

(a)

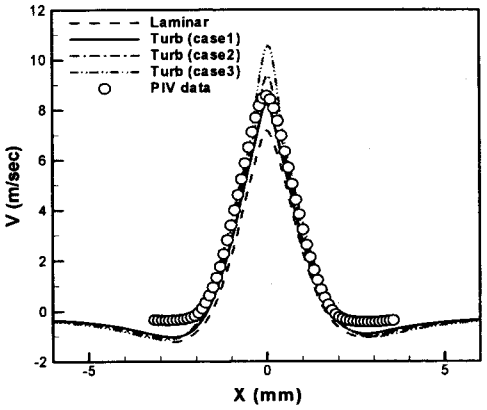

(b)

Fig. 4 Time-averaged V velocities: (a) y=0.3 mm, (b) y=4.0 mm.

displayed. PIV and LDV data show non-monotonic variations at the region of about 5-7 mm away from the slot exit. This variation implicates that there is a deceleration mechanism in that region. As the jet goes farther away, the velocity is decreased due to the turbulent dissipation. The present computational results reproduce this variation, though both position and magnitude are different from the experimental data. At the region Y>10 mm, the momentum in the vertical direction is not dissipated sufficiently. The discrepancy seems to be caused from insufficient turbulent dissipation of the turbulence model due to the stretched coarse mesh and the spatial discretization scheme used.

Figure 4 shows the time-averaged V velocities at y=0.3 and 4

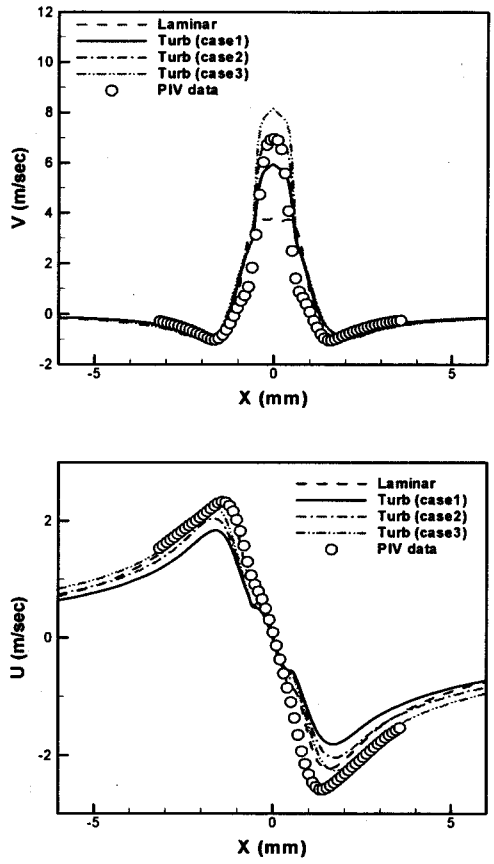

Fig. 5 Time-averaged V and U velocities at y=1.0 mm.

mm. Turbulent computations capture the jet width and the peak velocities at two positions. The laminar result gives a dip profile in the center region at y=0.3 mm. The present computational trend can be found also in the Fig. 5, which display the V and U velocities at y=1.0 mm. The spreading regions (the different slope region) in the V velocity distribution are caused from the vertical flow driven by the jet. The induced vortex outside the jet interacts with the synthetic jet and produces a roll up effect to the main stream. Regardless of the magnitude of the impulse, the resulting jet structures are nearly similar, which is also observed in the experimental study [1,9]. It is clear from Figs. 4 and 5 that the computational results capture most of the important features observed and agree well with the experimental data of Yao et al.

The phase-averaged U velocities and pressure fields at phase

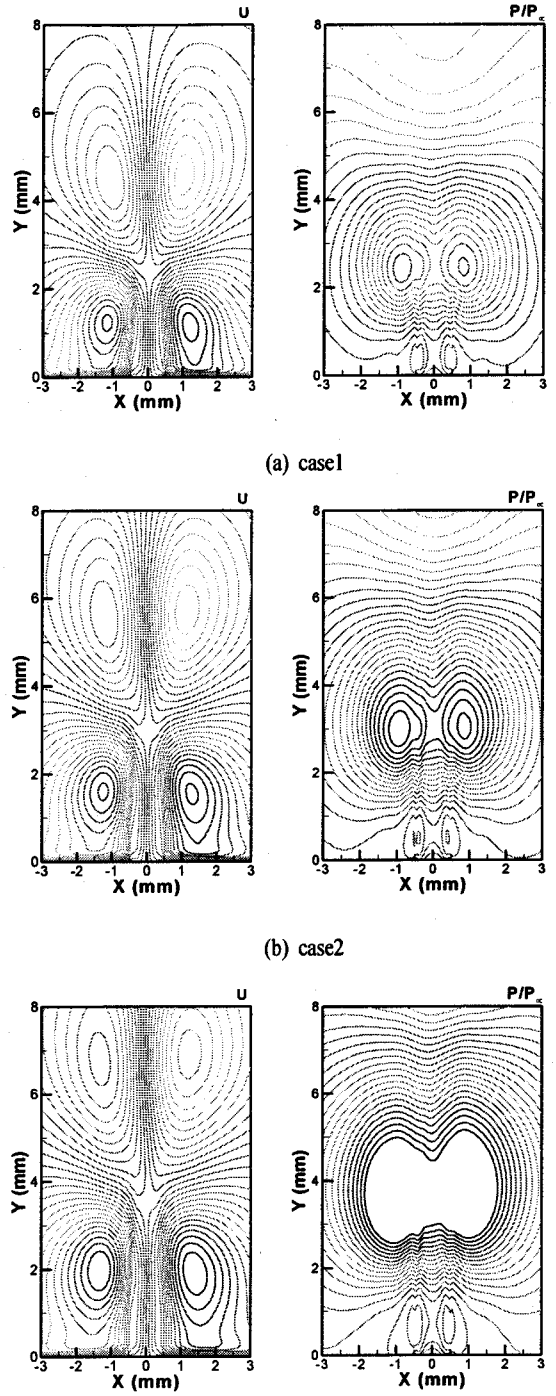

(a) case1

(b) case2

(c) case3

Fig. 6 Phase-averaged U velocity and gauge pressure contours at expulsion, phase=45 deg.

angle of 45 degrees at expulsion are displayed in Fig. 6. Near the slot exit the momentary fluid is ejected and rolled up, and thus the vortex pair is ultimately advected during the expulsion period. As shown, the center of the vortex moves away as the magnitude A in Eq. (3) of the diaphragm oscillation is increased. It is found that larger region of low pressure is located around zero U velocity position at centerline where the phase-averaged vertical speed approach to a peak. The jet flow experiences an adverse pressure gradient and the vertical velocity is consequently decelerated at this region. From this finding, the non-monotonic variation in V velocity shown in Fig. 3 can be explained by the existence of the low pressure region. The instantaneous effect of the pressure gradient is accumulated during a cycle and affects the vertical velocity distribution, which is related with the performance of the synthetic jet. The jet is primarily accelerated by the interaction with the induced vortices and locally decelerated by the region in low pressure. This is thought of as a kind of "flapping" of the time-dependent synthetic jet. Further investigation is needed for clarification.

4. Conclusion

The present computation for the synthetic jet flow captures flow physics well and agrees with the experimental data, including the width and the magnitude of the synthetic jet. The peak V velocity varies linearly with the maximum deflection of the vibrating diaphragm, whereas the structure of the jet is not affected by the magnitude. The present investigation for the phase-averaged flow field at expulsion stage gives an explanation to the local deceleration phenomena of the vertical velocity distribution.

참고문헌

[1] D. Auerhach, "Experiments on the trajectory and circulation of the starting vortex," *J. Fluid Mech.*, Vol. 183, 185 (1987)

[2] B. L. Smith and A. Glezer, "The Formation and Evolution of Synthetic Jets," *Phys. Fluids*, Vol. 10, 2281 (1998)

[3] V. N. Vatsa and E. Turkel, "Simulation of Synthetic Jets Using Unsteady Reynolds-Averaged Navier-Stokes Equations," *AIAA J.*, Vol. 44, 217 (2006)

[4] N. K. Yamaleev and M. H. Carpenter, "Quasi-one-Dimensional Model for Realistic Three-Dimensional Synthetic Jet Actuators," *AIAA J.*, Vol. 44, 208 (2006)

[5] C. L. Rumsey, T. B. Gatski, W. L. Sellers III, V. N. Vatsa and S. A. Viken, "Summary of the 2004 Computational Fluid Dynamics Validation Workshop on Synthetic Jets," *AIAA J.*, Vol. 44, 194 (2006)

[6] J. M. Weiss and W. A. Smith, "Preconditioning Applied to Variable and Constant Density Flows," *AIAA J.*, Vol. 33, 2050 (1995)

[7] S. H. Park and J. H. Kwon, "Preconditioned HLLE Method for Flows at All Mach Numbers," accepted for publication in AIAA J. (2006)

[8] S. H. Park and J. H. Kwon, "Implementation of k-ω Turbulence Models in an Implicit Multigrid Method," *AIAA J.*, Vol. 42, 1348 (2004)

[9] C. Yao, F. J. Chen, D. Neuhart and J. Harris, "Synthetic Jet Flow Field Database for CFD Validation," AIAA Paper 2004-2218 (2004)